JOC Article
pubs.acs.org/joc

Electron Transfer Properties of Alkoxyl Radicals. A Time-Resolved Kinetic Study of the Reactions of the *tert*-Butoxyl, Cumyloxyl, and Benzyloxyl Radicals with Alkyl Ferrocenes

Massimo Bietti,*[,†] Gino A. DiLabio,[‡] Osvaldo Lanzalunga,*[,§] and Michela Salamone[†]

[†]*Dipartimento di Scienze e Tecnologie Chimiche, Università "Tor Vergata", Via della Ricerca Scientifica, 1 I-00133 Rome, Italy,* [‡]*National Institute for Nanotechnology, National Research Council of Canada, 11421 Saskatchewan Drive, Edmonton, AB, Canada T6G 2M9, and* [§]*Dipartimento di Chimica, Sapienza Università di Roma and Istituto CNR di Metodologie Chimiche (IMC−CNR), Sezione Meccanismi di Reazione, c/o Dipartimento di Chimica, Sapienza Università di Roma, P. le A. Moro, 5 I-00185 Rome, Italy*

bietti@uniroma2.it; osvaldo.lanzalunga@uniroma1.it

Received May 12, 2010

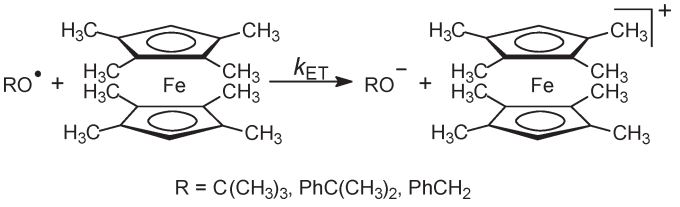

A time-resolved kinetic study on the reactions of the *tert*-butoxyl (*t*-BuO$^{\bullet}$), cumyloxyl (CumO$^{\bullet}$), and benzyloxyl (BnO$^{\bullet}$) radicals with alkylferrocenes has been carried out in MeCN solution. With all radicals, clear evidence for an electron transfer (ET) process has been obtained, and with the same ferrocene donor, the reactivity has been observed to increase in the order *t*-BuO$^{\bullet}$ < CumO$^{\bullet}$ < BnO$^{\bullet}$, with the difference in reactivity approaching 3 orders of magnitude on going from *t*-BuO$^{\bullet}$ to BnO$^{\bullet}$. With BnO$^{\bullet}$, an excellent fit to the Marcus equation has been obtained, from which a value of the reduction potential of BnO$^{\bullet}$ ($E^{\circ}_{\mathrm{BnO}^{\bullet}/\mathrm{BnO}^{-}}$ = 0.54 V/SCE) has been derived. The latter value appears, however, to be significantly higher than the previously determined reduction potential values for alkoxyl radicals and in contrast with the differences in the computed solution-phase electron affinities determined for *t*-BuO$^{\bullet}$, CumO$^{\bullet}$, and BnO$^{\bullet}$, indicating that the reaction of BnO$^{\bullet}$ with ferrocene donors may not be described in terms of a straightforward outer sphere ET mechanism. From these data, and taking into account the available value of the reduction potential for CumO$^{\bullet}$, a value of $E^{\circ}_{\mathrm{BnO}^{\bullet}/\mathrm{BnO}^{-}}$ = −0.10 V/SCE has been estimated. On the basis of computational evidence for the formation of a π-stacked prereaction complex in the reaction between BnO$^{\bullet}$ and DcMFc, an alternative ET mechanism is proposed for the reactions of both CumO$^{\bullet}$ and BnO$^{\bullet}$. In these cases, the delocalized nature of the unpaired electron allows for the aromatic ring to act as an electron relay by mediating the ET from the ferrocene donor to the formal oxygen radical center. This hypothesis is also in line with the observation that both BnO$^{\bullet}$ and CumO$^{\bullet}$ react with the ferrocene donors with rate constants that are in all cases at least 2 orders of magnitude higher than those measured for *t*-BuO$^{\bullet}$, wherein the radical is well-localized.

Introduction

Reactive free radicals play a detrimental role in biological systems, contributing to a variety of disease processes, and accordingly, the study of the mechanisms of action of potential antioxidants that are active against these species is the subject of intense investigation.[1] In particular, there is growing attention for the possible role of electron-transfer (ET) mechanisms in the radical-scavenging ability of antioxidant species, as it is now generally accepted that ET can play an important role in a variety of formal hydrogen atom transfer processes from easily oxidizable substrates

(1) Halliwell, B.; Gutteridge, J. M. C. *Free Radicals in Biology and Medicine*, 4th ed.; Oxford University Press: Oxford, 2007.

DOI: 10.1021/jo100931a Published on Web 08/12/2010

(i.e., phenols and tertiary amines) to radical or radical-like[2] species.[3−13] Along this line, the assessment of the ET properties of the free radicals involved in these processes appears to be of great importance, and several studies have dealt with the ET reactivity of important classes of free radicals such as peroxyl,[14−21] phenoxyl,[9,22−26] and *N*-oxyl radicals.[12,27−30] Very limited information is instead available on the redox properties and ET reactivity of alkoxyl radicals,[31−34] one of the main classes of oxygen-centered radicals. These species are involved in a variety of synthetically useful procedures[35] and play a key role in several chemical and biological processes, such as the photooxidation of hydrocarbons in the atmosphere,[36] lipid peroxidation,[1] and the antimalarial action of natural endoperoxides.[37]

Recently, while conducting a time-resolved kinetic study on the ET reactions of the phthalimide-*N*-oxyl radical (PINO) with substituted ferrocene donors,[30] we observed that the decay of the cumyloxyl radical (employed for the generation of PINO by hydrogen atom abstraction (HAT) from *N*-hydroxyphthalimide (NHPI)) was significantly accelerated by the presence of easily oxidizable ferrocenes such as 1,1′,2,2′,3,3′,4,4′-octamethylferrocene (OMFc) and decamethylferrocene (DcMFc), clearly indicating that the ferrocene donor competes with NHPI for the reaction with the cumyloxyl radical and suggesting, in particular, the occurrence of an ET reaction between the cumyloxyl radical and both OMFc and DcMFc.

This observation prompted us to investigate more in detail these processes in order to acquire quantitative information on the intrinsic ET reactivity of alkoxyl radicals, and for this purpose we have carried out a time-resolved kinetic study on the reactions of three of the most representative alkoxyl radicals, namely the *tert*-butoxyl (*t*-BuO$^\bullet$), cumyloxyl (CumO$^\bullet$), and benzyloxyl (BnO$^\bullet$) radicals, with ferrocene (FcH), ethylferrocene (EtFc), 1,1′-dimethylferrocene (DMFc), 1,1′,2,2′,3,3′,4,4′-octamethylferrocene (OMFc), and decamethylferrocene (DcMFc), whose structures are displayed in Chart 1.

Results and Discussion

t-BuO$^\bullet$, CumO$^\bullet$, and BnO$^\bullet$ have been generated by 266 nm laser flash photolysis (LFP) of MeCN solutions (T = 25 °C) containing di-*tert*-butyl, dicumyl, and dibenzyl peroxide, respectively (eq 1).

$$\mathrm{RO{-}OR} \xrightarrow[266\ \mathrm{nm}]{h\nu} 2\ \mathrm{RO}^\bullet \qquad (1)$$

R = $C(CH_3)_3$, $PhC(CH_3)_2$, $PhCH_2$

As described previously, in MeCN solution *t*-BuO$^\bullet$ is characterized by a relatively weak UV band centered at 280 nm,[38,39] while CumO$^\bullet$ and BnO$^\bullet$ are characterized by a broad absorption band in the visible region of the spectrum centered at 485 and 460 nm, respectively.[39,40] Under these conditions, *t*-BuO$^\bullet$ and CumO$^\bullet$ decay mainly by C−CH$_3$ β-scission,[38,39,41] while the decay of BnO$^\bullet$ can be

(2) For a definition, see: Mayer, J. M. *Acc. Chem. Res.* **1998**, *31*, 441–450.
(3) Gunay, A.; Theopold, K. H. *Chem. Rev.* **2010**, *110*, 1060–1081.
(4) Valgimigli, L.; Amorati, R.; Petrucci, S.; Pedulli, G. F.; Hu, D.; Hanthorn, J. J.; Pratt, D. A. *Angew. Chem., Int. Ed.* **2009**, *48*, 8348–8351.
(5) Costentin, C. *Chem. Rev.* **2008**, *108*, 2145–2179.
(6) Tishchenko, O.; Truhlar, D. G.; Ceulemans, A.; Nguyen, M. T. *J. Am. Chem. Soc.* **2008**, *130*, 7000–7010.
(7) Huynh, M. H. V.; Meyer, T. J. *Chem. Rev.* **2007**, *107*, 5004–5064.
(8) DiLabio, G. A.; Johnson, E. R. *J. Am. Chem. Soc.* **2007**, *129*, 6199–6203.
(9) Litwinienko, G.; Ingold, K. U. *Acc. Chem. Res.* **2007**, *40*, 222–230.
(10) Derat, E.; Shaik, S. *J. Am. Chem. Soc.* **2006**, *128*, 13940–13949.
(11) Mayer, J. M.; Hrovat, D. A.; Thomas, J. L.; Borden, W. T. *J. Am. Chem. Soc.* **2002**, *124*, 11142–11147.
(12) (a) Baciocchi, E.; Bietti, M.; Lanzalunga, O.; Lapi, A.; Raponi, D. *J. Org. Chem.* **2010**, *75*, 1378–1385. (b) Baciocchi, E.; Bietti, M.; Gerini, M. F.; Lanzalunga, O. *J. Org. Chem.* **2005**, *70*, 5144–5149.
(13) Meunier, B.; de Visser, S. P.; Shaik, S. *Chem. Rev.* **2004**, *104*, 3947–3980.
(14) Jomová, K.; Kysel, O.; Madden, J. C.; Morris, H.; Enoch, S. J.; Budzak, S.; Young, A. J.; Cronin, M. T. D.; Mazur, M.; Valko, M. *Chem. Phys. Lett.* **2009**, *478*, 266–270.
(15) Goldstein, S.; Samuni, A. *J. Phys. Chem. A* **2007**, *111*, 1066–1072.
(16) Fukuzumi, S.; Shimoosako, K.; Suenobu, T.; Watanabe, Y. *J. Am. Chem. Soc.* **2003**, *125*, 9074–9082.
(17) Brinck, T.; Lee, H.-N.; Jonsson, M. *J. Phys. Chem. A* **1999**, *103*, 7094–7104.
(18) Das, T. N.; Dhanasekaran, T.; Alfassi, Z. B.; Neta, P. *J. Phys. Chem. A* **1998**, *102*, 280–284.
(19) Jonsson, M. *J. Phys. Chem.* **1996**, *100*, 6814–6818.
(20) Alfassi, Z. B.; Khaikin, G. I.; Neta, P. *J. Phys. Chem.* **1995**, *99*, 265–268.
(21) Jovanovic, S. V.; Jankovic, I.; Josimovic, L. *J. Am. Chem. Soc.* **1992**, *114*, 9018–9021.
(22) Omura, K. *J. Org. Chem.* **2008**, *73*, 858–867.
(23) Grampp, G.; Landgraf, S.; Mureşanu, C. *Electrochim. Acta* **2004**, *49*, 537–544.
(24) Steenken, S.; Neta, P. In *The Chemistry of Phenols*; Rappoport, Z., Ed.; John Wiley & Sons: New York, 2003; Chapter 16, pp 1107−1152.
(25) Itoh, S.; Kumei, H.; Nagatomo, S.; Kitagawa, T.; Fukuzumi, S. *J. Am. Chem. Soc.* **2001**, *123*, 2165–2175.
(26) Armstrong, D. A.; Sun, Q.; Schuler, R. H. *J. Phys. Chem.* **1996**, *100*, 9892–9899.
(27) Baciocchi, E.; Bietti, M.; Di Fusco, M.; Lanzalunga, O.; Raponi, D. *J. Org. Chem.* **2009**, *74*, 5576–5583.
(28) Galli, C.; Gentili, P.; Lanzalunga, O. *Angew. Chem., Int. Ed.* **2008**, *47*, 4790–4796.
(29) Manda, S.; Nakanishi, I.; Ohkubo, K.; Yakumaru, H.; Matsumoto, K.; Ozawa, T.; Ikota, N.; Fukuzumi, S.; Anzai, K. *Org. Biomol. Chem.* **2007**, *5*, 3951–3955.
(30) Baciocchi, E.; Bietti, M.; Di Fusco, M.; Lanzalunga, O. *J. Org. Chem.* **2007**, *72*, 8748–8754.
(31) (a) Magri, D. C.; Workentin, M. S. *Chem.—Eur. J.* **2008**, *14*, 1698–1709. (b) Donkers, R. L.; Workentin, M. S. *J. Am. Chem. Soc.* **2004**, *126*, 1688–1698. (c) Donkers, R. L.; Tse, J.; Workentin, M. S. *Chem. Commun.* **1999**, 135–136.
(32) (a) Donkers, R. L.; Maran, F.; Wayner, D. D. M.; Workentin, M. S. *J. Am. Chem. Soc.* **1999**, *121*, 7239–7248. (b) Antonello, S.; Musumeci, M.; Wayner, D. D. M.; Maran, F. *J. Am. Chem. Soc.* **1997**, *119*, 9541–9549. (c) Workentin, M. S.; Maran, F.; Wayner, D. D. M. *J. Am. Chem. Soc.* **1995**, *117*, 2120–2121.
(33) Mihaljević, B.; Ražem, D. *Radiat. Phys. Chem.* **2003**, *67*, 269–274.
(34) Ledwith, A. *Acc. Chem. Res.* **1972**, *5*, 133–139.
(35) See, for example: (a) Zhu, H.; Wickenden, J. G.; Campbell, N. E.; Leung, J. C. T.; Johnson, K. M.; Sammis, G. M. *Org. Lett.* **2009**, *11*, 2019–2022. (b) Xu, W.; Zou, J.-P.; Mu, X.-J.; Zhang, W. *Tetrahedron Lett.* **2008**, *49*, 7311–7314. (c) Francisco, C. G.; González, C. C.; Kennedy, A. R.; Paz, N. R.; Suárez, E. *Chem.—Eur. J.* **2008**, *14*, 6704–6712.
(36) Orlando, J. J.; Tyndall, G. S.; Wallington, T. J. *Chem. Rev.* **2003**, *103*, 4657–4689.
(37) See, for example: (a) Chaturvedi, D.; Goswami, A.; Saikia, P. P.; Barua, N. C.; Rao, P. G. *Chem. Soc. Rev.* **2010**, *39*, 435–454. (b) Robert, A.; Bonduelle, C.; Laurent, S. A.-L.; Meunier, B. *J. Phys. Org. Chem.* **2006**, *19*, 562–569. (c) Posner, G. H.; O'Neill, P. M. *Acc. Chem. Res.* **2004**, *37*, 397–404.
(38) Tsentalovich, Y. P.; Kulik, L. V.; Gritsan, N. P.; Yurkovskaya, A. V. *J. Phys. Chem. A* **1998**, *102*, 7975–7980.
(39) Baciocchi, E.; Bietti, M.; Salamone, M.; Steenken, S. *J. Org. Chem.* **2002**, *67*, 2266–2270.
(40) (a) Avila, D. V.; Ingold, K. U.; Di Nardo, A. A.; Zerbetto, F.; Zgierski, M. Z.; Lusztyk, J. *J. Am. Chem. Soc.* **1995**, *117*, 2711–2718. (b) Avila, D. V.; Lusztyk, J.; Ingold, K. U. *J. Am. Chem. Soc.* **1992**, *114*, 6576–6577.
(41) Avila, D. V.; Brown, C. E.; Ingold, K. U.; Lusztyk, J. *J. Am. Chem. Soc.* **1993**, *115*, 466–470.

CHART 1

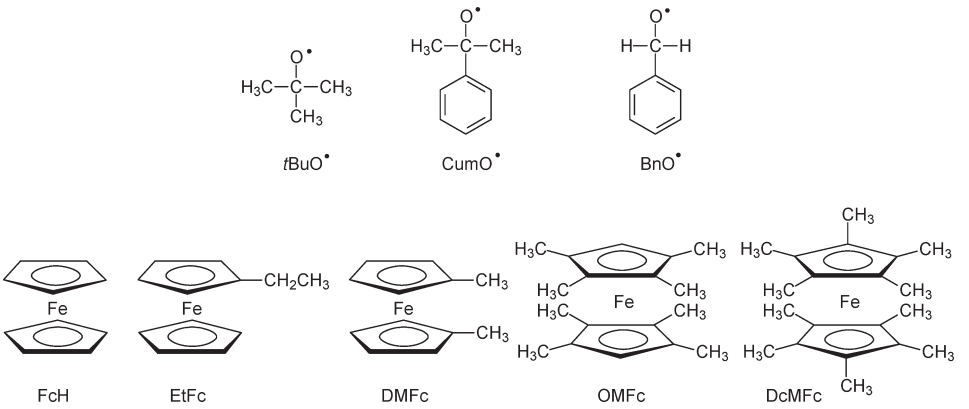

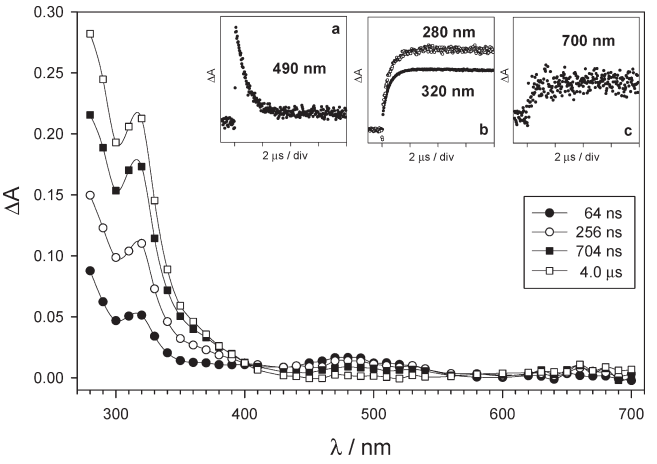

FIGURE 1. Time-resolved absorption spectra observed after 266 nm LFP of an argon-saturated MeCN solution (T = 25 °C) containing dicumyl peroxide (10.0 mM) and decamethylferrocene (0.37 mM) at 64 ns (filled circles), 256 ns (empty circles), 704 ns (filled squares), and 4.0 μs (empty squares) after the 8 ns, 10 mJ laser pulse. Insets: (a) Decay of the cumyloxyl radical monitored at 490 nm; (b and c) Corresponding buildup of absorption at 280 (b: empty circles), 320 (b: filled circles) and 700 nm (c) assigned to the formation of the decamethylferrocenium ion.

mainly attributed to hydrogen atom abstraction from the solvent.[42,43]

The reactions of the alkoxyl radicals with the ferrocene donors were studied in MeCN by LFP. Figure 1 shows the time-resolved absorption spectra observed after 266 nm LFP of an argon-saturated MeCN solution (T = 25 °C) containing dicumyl peroxide and DcMFc. The spectrum recorded 64 ns after the laser pulse (filled circles) is characterized by the presence of the characteristic CumO• band centered at 485 nm. The decay of this band (inset a), which is accelerated by the presence of DcMFc, is accompanied by a corresponding buildup of absorption at 280, 320, and 700 nm (insets b and c). Two isosbestic points can be identified at 400 and 560 nm. These absorption bands are assigned to the decamethylferrocenium ion ($DcMFc^+$) by comparison with literature data[44] and with the spectrum of $DcMFc^+PF_6^-$, synthesized according to a literature procedure (see the Supporting Information, Figure S1).[45]

The formation of $DcMFc^+$ clearly indicates the occurrence of an ET reaction from DcMFc to CumO• (eq 2).

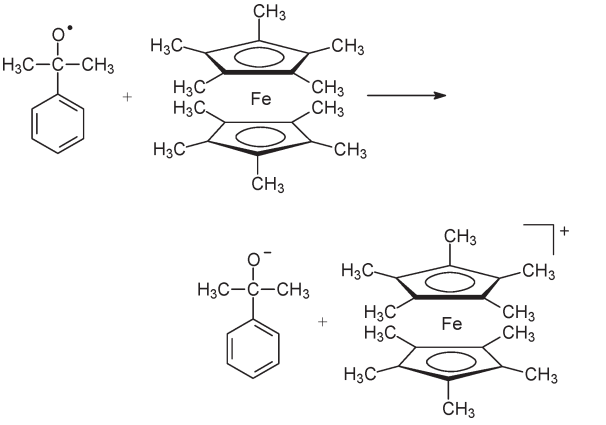

(2)

Analogous results were obtained in the reactions of the three alkoxyl radicals with the ferrocene donors (see below), showing in all cases the buildup of the pertinent ferrocenium bands, indicative of the occurrence of an ET reaction. The time-resolved spectra observed after reaction of *t*-BuO• with OMFc and DcMFc, of CumO• with OMFc, and of BnO• with DMFc are reported in the Supporting Information (Figures S2−S5).

Kinetic studies were carried out by LFP following the buildup of the ferrocenium ions between 300 and 330 nm and, in the reactions of CumO• and BnO•, also by following the decay of the alkoxyl radical visible absorption bands. With CumO• the kinetic study was limited to DMFc, OMFc and DcMFc because FcH and EtFc were not sufficiently reactive to be studied under these conditions. For the same reason, with *t*-BuO• the kinetic study was limited to OMFc and DcMFc.

When the observed rate constants (k_{obs}) were plotted against the ferrocene concentration, excellent linear

(42) Konya, K. G.; Paul, T.; Lin, S.; Lusztyk, J.; Ingold, K. U. *J. Am. Chem. Soc.* **2000**, *122*, 7518–7527.

(43) BnO• undergoes a rapid 1,2-H-atom shift reaction in water and alcohols (see ref 42). Accordingly, in MeCN the decay of this radical can be accelerated by the presence of small amounts of water.

(44) Frey, J. E.; Du Pont, L. E.; Puckett, J. J. *J. Org. Chem.* **1994**, *59*, 5386–5392.

(45) Yang, E. S.; Chan, M.-S.; Wahl, A. C. *J. Phys. Chem.* **1980**, *84*, 3094–3099.

TABLE 1. Second-Order Rate Constants for the Reactions of *t*-BuO•, CumO•, and BnO• with Ferrocene and Alkylferrocenes (k_{ET}) Measured in MeCN at $T = 25$ °C[a] and Oxidation Potentials of the Ferrocene Donors

		$k_{ET}/M^{-1}s^{-1}$		
	E°[b]	*t*-BuO•[c]	CumO•[c]	BnO•[c]
FcH	0.41			6.3×10^7
EtFc	0.34			2.4×10^8
				2.6×10^8[d]
DMFc	0.29		1.0×10^8	5.2×10^8
OMFc	−0.02	9.6×10^6	2.0×10^9[e]	7.5×10^9[f]
			1.1×10^9[d,e]	
DcMFc	−0.10	2.5×10^7	4.0×10^9	1.1×10^{10}
			2.0×10^9[d]	

[a]Determined from the slope of the k_{obs} vs [ferrocene] plots. Average of at least two values. Error < 10%. k_{obs} was measured following the buildup of the pertinent ferrocenium ion (at 300 nm for Fc^+, $EtFc^+$, and $DMFc^+$, 330 nm for $OMFc^+$, 320 nm for $DcMFc^+$). [b]V vs SCE in MeCN. Taken from ref 30. [c]Generated by 266 nm LFP of the parent peroxide. [d]k_{obs} was measured following the decay of the alkoxyl radical visible absorption band. [e]No significant kinetic effect was observed when 1 M H_2O or 1 M HFIP was added. [f]The reaction was studied both in anhydrous and spectroscopic grade MeCN, and no significant kinetic effect was observed.

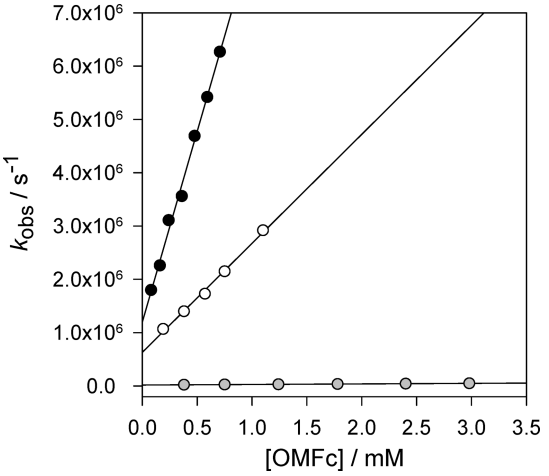

FIGURE 2. Plots of the observed rate constant (k_{obs}) against [OMFc] for the reactions of the benzyloxyl (black circles), cumyloxyl (white circles), and *tert*-butoxyl radicals (gray circles), measured in argon-saturated MeCN solution at $T = 25$ °C, following the buildup of $OMFc^+$ at 330 nm. From the linear regression analysis: BnO• + OMFc $k_{ET} = 7.2 \times 10^9$ M^{-1} s^{-1}, $r^2 = 0.9941$. CumO• + OMFc $k_{ET} = 2.0 \times 10^9$ M^{-1} s^{-1}, $r^2 = 0.9957$. *t*-BuO• + OMFc $k_{ET} = 1.0 \times 10^7$ M^{-1} s^{-1}, $r^2 = 0.9990$.

dependencies were observed, and the second-order rate constants for the one-electron oxidation of the ferrocene donors by the alkoxyl radicals (k_{ET}) were obtained from the slopes of these plots. All the kinetic data are collected in Table 1. Also included are the redox potentials of the ferrocene donors. The plots of k_{obs} vs [OMFc] for the reactions of BnO•, CumO•, and *t*-BuO•, are shown in Figure 2. Additional plots for the reactions investigated are reported in the Supporting Information (Figures S6−S13).

The data displayed in Table 1 show that the k_{ET} values increase by decreasing the oxidation potential of the ferrocene donor, as expected for an ET process, varying, in the case of BnO•, from 6.3×10^7 to 1.1×10^{10} M^{-1} s^{-1} on going from FcH to DcMFc. In the reactions with OMFc and DcMFc an almost 3 orders of magnitude increase in reactivity is also observed in the alkoxyl radical series, following the order *t*-BuO• < CumO• < BnO•. This reactivity order can be reasonably ascribed to differences in the oxidizing properties of the three alkoxyl radicals (see below).

It is generally assumed that *t*-BuO• and CumO• display similar reactivities in HAT processes.[46] Along this line, the occurrence of an HAT reaction from the ferrocene alkyl substituents to CumO• (and BnO•) can be ruled out on the basis of the >100-fold increase in reactivity observed in the reactions of *t*-BuO• and CumO• with the same ferrocene donor (namely OMFc and DcMFc). For what concerns instead *t*-BuO•, the low reactivity observed in the reaction with DMFc (that could not be investigated on the microsecond time scale), coupled, as mentioned above, with the observation of the pertinent ferrocenium bands following its reaction with OMFc and DcMFc (Supporting Information, Figures S2 and S3), support the hypothesis that also the latter two reactions follow an ET mechanism. In agreement with this hypothesis are also the relatively low rate constants ($< 10^6$ M^{-1} s^{-1}) measured for HAT from methyl benzenes to *t*-BuO•.[47−51]

Very limited information is presently available on the redox properties of alkoxyl radicals, the given data being obtained by means of thermochemical calculations or from voltammetry of the alkoxide anions.[32] Along this line, in an attempt to quantify the ET properties of the alkoxyl radicals examined in our study, and in order to provide a mechanistic rationale for these processes, we have considered it worthwhile to analyze the kinetic data for the reactions of BnO• with alkyl ferrocenes (the more extended series of data reported in Table 1, spanning more than 2 orders of magnitude) in the framework of the Marcus theory for outer sphere ET.[54] The Marcus equation provides a quantitative relationship among λ, $\Delta G^{\ddagger}$, and $\Delta G^{\circ\prime}$ (eq 3), where $\Delta G^{\ddagger}$ is the activation free energy for the ET step, $\Delta G^{\circ\prime}$ is the standard free energy for the same step corrected for the electrostatic interaction arising from the charge variation in the reactants upon ET, and λ is the reorganization energy that is the energy required for the adjustments in

(46) See, for example: (a) Valgimigli, L.; Banks, J. T.; Ingold, K. U.; Lusztyk, J. *J. Am. Chem. Soc.* **1995**, *117*, 9966–9971. (b) Sheeller, B.; Ingold, K. U. *J. Chem. Soc., Perkin Trans. 2* **2001**, 480–486. (c) Baignée, A.; Howard, J. A.; Scaiano, J. C.; Stewart, L. C. *J. Am. Chem. Soc.* **1983**, *105*, 6120–6123.

(47) Finn, M.; Friedline, R.; Suleman, N. K.; Wohl, C. J.; Tanko, J. M. *J. Am. Chem. Soc.* **2004**, *126*, 7578–7584.

(48) Paul, H.; Small, R. D., Jr.; Scaiano, J. C. *J. Am. Chem. Soc.* **1978**, *100*, 4520–4527.

(49) It is, however, important to point out that a rate constant $k_H = 7.3 \times 10^6$ M^{-1} s^{-1} has been recently measured in MeCN for the hydrogen atom abstraction reaction from hexamethylbenzene by CumO• (see ref 50). On the basis of this value, it is not possible to exclude that the reactions of *t*-BuO• with both OMFc and DcMFc proceed, at least in part, by hydrogen atom abstraction from the ferrocene methyl groups.

(50) Koner, A. L.; Pischel, U.; Nau, W. M. *Org. Lett.* **2007**, *9*, 2899–2902.

(51) For a critical discussion on the factors controlling reactivity in hydrogen abstractions by radicals, see, for example, refs 6, 52, and 53.

(52) (a) Wu, A.; Mader, E. A.; Datta, A.; Hrovat, D. A.; Borden, W. T.; Mayer, J. M. *J. Am. Chem. Soc.* **2009**, *131*, 11985–11997. (b) Isborn, C.; Hrovat, D. A.; Borden, W. T.; Mayer, J. M.; Carpenter, B. K. *J. Am. Chem. Soc.* **2005**, *127*, 5794–5795. (c) Roth, J. P.; Yoder, J. C.; Won, T.-J.; Mayer, J. M. *Science* **2001**, *294*, 2524–2526. (d) Roth, J. P.; Lovell, S.; Mayer, J. M. *J. Am. Chem. Soc.* **2000**, *122*, 5486–5498.

(53) (a) Zavitsas, A. A. *J. Am. Chem. Soc.* **1998**, *120*, 6578–6586. (b) Zavitsas, A. A.; Chatgilialoglu, C. *J. Am. Chem. Soc.* **1995**, *117*, 10645–10654. (c) Zavitsas, A. A.; Melikian, A. A. *J. Am. Chem. Soc.* **1975**, *97*, 2757–2763.

(54) The same approach could not be applied to *t*-BuO• and CumO• due to the limited kinetic information obtained for their reactions with alkylferrocenes.

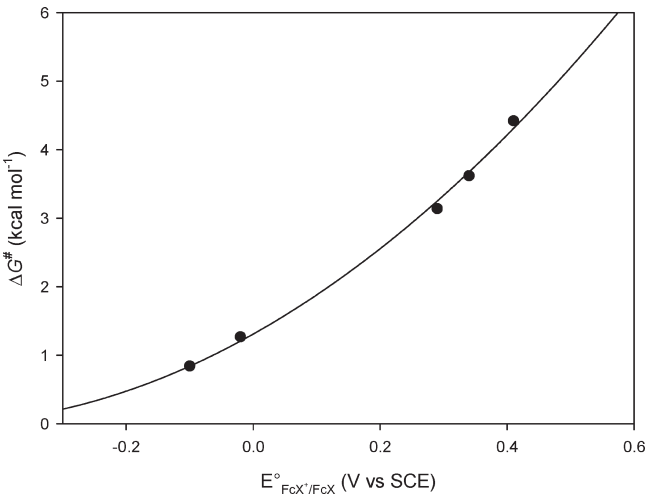

FIGURE 3. Plot of $\Delta G^{\ddagger}$ vs $E^{\circ}_{FcX^{+}/FcX}$ for the reactions of $BnO^{\bullet}$ with alkyl ferrocenes in MeCN. Circles correspond to the experimental values; the curve has been calculated according to eq 7 with $E^{\circ}_{BnO\bullet/BnO^{-}} = 0.54$ V vs SCE and $\lambda = 25.7$ kcal mol^{-1}.

nuclear geometry and solvation shell which make the ET possible.[55,56]

$$\Delta G^{\ddagger} = \frac{\lambda}{4}\left(1+\frac{\Delta G^{\circ\prime}}{\lambda}\right)^{2} \tag{3}$$

The $\Delta G^{\ddagger}$ values are obtained from the ET rate constant (k_{ET}) displayed in Table 1 and the diffusion rate constant (k_d) according to eq 4, where Z is the collision frequency taken as 10^{11} M^{-1} s^{-1},[56] and in MeCN $k_d = 2.0 \times 10^{10}$ M^{-1} s^{-1}.[57] The $\Delta G^{\ddagger}$ values thus obtained are listed in the Supporting Information, Table S1.

$$\Delta G^{\ddagger} = RT \ln[Z(k_{ET}{}^{-1} - k_d{}^{-1})] \tag{4}$$

$\Delta G^{\circ\prime}$ values are given by eq 5 where ΔG° is the standard free energy for the ET process obtained from eq 6 (where in turn the $E^{\circ}_{FcX^{+}/FcX}$ values are given in Table 1), Z_1 and Z_2 are the charges of the oxidant (0) and of the alkylferrocene (0), respectively, e is the electron charge, r_{12} is the distance between $BnO^{\bullet}$ and the ferrocene in the encounter complex (taken as 5.55 Å, calculated using dispersion-corrected density-functional theory;[58,59] for the details see the Supporting Information), D is the dielectric constant of the medium (35.94 for acetonitrile)[60], and f is a factor which accounts for the ionic strength ($f = 1$ for $\mu = 0$).

$$\Delta G^{\circ\prime} = \Delta G^{\circ} + \frac{(Z_1 - Z_2 - 1)e^2 f}{Dr_{12}} \tag{5}$$

$$\Delta G^{\circ} = 23.06[E^{\circ}_{FcX^{+}/FcX} - E^{\circ}_{BnO^{\bullet}/BnO^{-}}] \tag{6}$$

By combining eqs 5 and 6 with eq 3, eq 7 is obtained, which relates ΔG° to the (unknown) reduction potential of the benzyloxyl radical ($E^{\circ}_{BnO\bullet/BnO-}$).

$$\Delta G^{\ddagger} = \frac{\lambda}{4}\left(1+\frac{23.06[E^{\circ}_{FcX^{+}/FcX} - E^{\circ}_{BnO^{\bullet}/BnO^{-}}] - \dfrac{e^2 f}{Dr_{12}}}{\lambda}\right)^{2} \tag{7}$$

Nonlinear least-squares curve fitting of the experimental data has been carried out using $E^{\circ}_{BnO\bullet/BnO-}$ and the reorganization energy λ as adjustable parameters. An excellent fit of the experimental data to eq 7 has been obtained ($r^2 = 0.999$), and the results are displayed in Figure 3. Values of $E^{\circ}_{BnO\bullet/BnO-} = 0.54$ V vs SCE and of $\lambda = 25.7$ kcal mol^{-1} (which represents the overall (reactants and solvent) reorganization energy associated with the transfer of one electron from alkylferrocenes to $BnO^{\bullet}$) have been derived.

However, the $BnO^{\bullet}$ reduction potential derived from this approach is significantly higher than those available in the literature (in MeCN) for both *t*-$BuO^{\bullet}$ and $CumO^{\bullet}$, determined by means of thermochemical calculations ($E^{\circ}_{t\text{-}BuO\bullet/t\text{-}BuO-} = -0.30$ V/SCE)[32c] and voltammetry of the cumyloxide anion ($E^{\circ}_{CumO\bullet/CumO-} = -0.19$ V/SCE).[32a] Even though it is reasonable to assume that the oxidizing properties of the latter two radicals are lower than that of $BnO^{\bullet}$, the resulting differences appear far too high to be accounted for on the basis of our kinetic data. Along this line, we have calculated the solvent-phase (MeCN) electron affinities (EAs) for *t*-$BuO^{\bullet}$, $CumO^{\bullet}$, and $BnO^{\bullet}$ (for details, see the Supporting Information) and find $\Delta EA(CumO^{\bullet} - t\text{-}BuO^{\bullet}) = 0.13$ V in excellent agreement with the analogous ΔE° value from literature sources ($\Delta E^{\circ} = 0.11$ V),[32a,c] implying that our calculations are in accord with thermochemical and voltammetry data and supporting the assumption that differences in solvent-phase electron affinities parallel differences in reduction potential. However, the calculated $\Delta EA(BnO^{\bullet} - CumO^{\bullet}) = 0.09$ V is in very poor agreement with the ΔE° between these two radicals when we use the $BnO^{\bullet}$ reduction potential value derived from our Marcus-type analysis described above ($\Delta E^{\circ} = 0.73$ V). A reasonable approximation to $E^{\circ}_{BnO\bullet/BnO-}$ can be obtained by combining our calculated $\Delta EA(BnO^{\bullet} - CumO^{\bullet}) = 0.09$ V with the literature value for the reduction potential of $CumO^{\bullet}$ ($E^{\circ}_{CumO\bullet/CumO-} = -0.19$ V/SCE) to give $E^{\circ}_{BnO\bullet/BnO-} = -0.10$ V/SCE. This very large difference in reduction potential raises some doubts about the straightforward applicability of a Marcus-type analysis to the reactions between $BnO^{\bullet}$ and the ferrocene donors, indicating that this process can probably not be described in terms of an outer sphere ET mechanism.[61]

To obtain additional insights into these reactions, we modeled the $BnO^{\bullet}$ + DcMFc (Figure 4a) and *t*-$BuO^{\bullet}$ + DcMFc (Figure 4b) prereaction complexes using dispersion-corrected density functional theory[58,59] (see the Supporting Information for additional computational details). Figure 4

(55) (a) Marcus, R. A. *Angew. Chem., Int. Ed. Engl.* **1993**, *32*, 1111–1121. (b) Marcus, R. A.; Sutin, N. *Biochim. Biophys. Acta* **1985**, *811*, 265–322.
(56) Nelsen, S. F.; Pladziewicz, J. R. *Acc. Chem. Res.* **2002**, *35*, 247–254.
(57) Fukuzumi, S.; Nakanishi, I.; Tanaka, K.; Suenobu, T.; Tabard, A.; Guilard, R.; Van Caemelbecke, E.; Kadish, K. M. *J. Am. Chem. Soc.* **1999**, *121*, 785–790.
(58) DiLabio, G. A. *Chem. Phys. Lett.* **2008**, *455*, 348–353.
(59) Mackie, I. D.; DiLabio, G. A. *J. Phys. Chem. A* **2008**, *112*, 10968–10976.
(60) Reichardt, C. *Solvents and Solvent Effects in Organic Chemistry*, 3rd ed.; Wiley-VCH: Weinheim, 2003.

(61) The observation that 1 M H_2O or 1 M HFIP had no effect on the rate constant for reaction of $CumO^{\bullet}$ with OMFc (see Table 1) appears also to be in contrast with an outer sphere ET mechanism. Further studies are underway in our laboratories to provide a better understanding of the role of solvent effects on these processes.

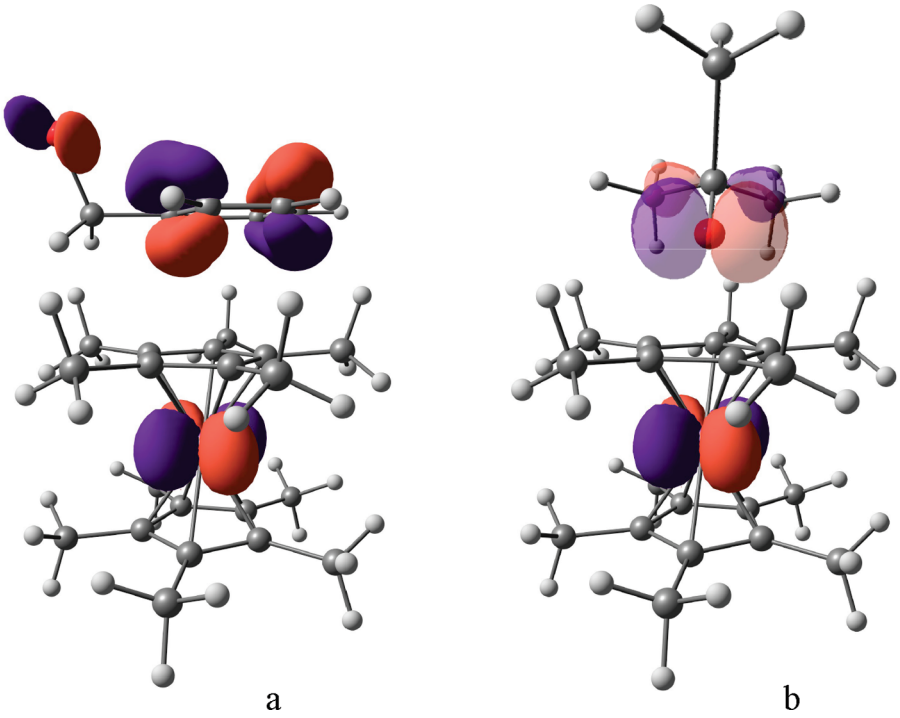

FIGURE 4. Calculated structures of the (a) $BnO^{\bullet}$−DcMFc and (b) *t*-$BuO^{\bullet}$−DcMFc prereaction complexes. Overlaid on the structures are the DcMFc highest occupied molecular orbital and the singly occupied molecular orbital of the radicals. The relative phases of the orbitals are differentiated by red and blue. The SOMO of *t*-$BuO^{\bullet}$ is shown as transparent in order to facilitate viewing.

illustrates the highest occupied molecular orbital (HOMO) of DcMFc and the singly occupied molecular orbitals (SOMO) associated with the radicals. Figure 4a reveals a situation where $BnO^{\bullet}$ + DcMFc form a π-stacked prereaction complex. The orbitals illustrate that ET between these species will occur from a predominantly Fe d-orbital of DcMFc to a delocalized orbital on $BnO^{\bullet}$. The delocalized nature of the $BnO^{\bullet}$ SOMO ensures that the electron from DcMFc can transfer to any part of the radical and will be able to pair up with the (formal) unpaired electron on the O atom. In other words, the benzyloxyl radical aromatic ring can act as an electron relay, shuttling the electron from the ferrocene donor to the oxygen atom. A similar mechanism will be operative in the ET reactions involving $CumO^{\bullet}$ and has been implicated in certain proton-coupled electron-transfer reactions.[8] On the other hand, the SOMO of *t*-$BuO^{\bullet}$ is highly localized (see Figure 4b), and it is necessary for the transient electron to be transferred directly to the O center. It is therefore quite clear that electron transfer reactions involving delocalized radicals, viz., $CumO^{\bullet}$ and $BnO^{\bullet}$, with ferrocenes have considerably different dynamics than those involving localized radicals such as *t*-$BuO^{\bullet}$.

In agreement with this hypothesis is also the observation that, with the same ferrocene donor, a ≤5-fold increase in reactivity is observed on going from $CumO^{\bullet}$ to $BnO^{\bullet}$ (see Table 1), whereas both these radicals react with rate constants that are in all cases at least 2 orders of magnitude higher than those measured for the corresponding reactions of *t*-$BuO^{\bullet}$, where this interaction is clearly not possible. In order to obtain additional information on these important processes, and to provide support to this mechanistic hypothesis, computational and experimental studies are currently under way in our laboratories.[62]

Experimental Section

Materials. Spectroscopic-grade acetonitrile was used in the kinetic experiments. Commercial samples of ferrocene (FcH), ethylferrocene (EtFc), 1,1′-dimethylferrocene (DMFc), 1,1′,2,2′,3,3′,4,4′-octamethylferrocene (OMFc), and decamethylferrocene (DcMFc) were further purified by sublimation (FcH, DMFc, OMFc, and DcMFc) or by column chromatography on silica gel using toluene as eluent (EtFc).

Dicumyl peroxide and di-*tert*-butyl peroxide were of the highest commercial quality available and were used as received. Dibenzyl peroxide was prepared in small portions by reaction of KO_2 with benzyl bromide in dry benzene, in the presence of 18-crown-6 ether, according to a previously described procedure.[42,63] The product was purified by column chromatography (silica gel, eluent hexane/dichloromethane 1:1) and identified by ^{1}H NMR. ^{1}H NMR ($CDCl_3$):[42] δ 7.34 (s, 10H, ArH), 4.95 (s, 4H, CH_2).

Decamethylferrocenium hexafluorophosphate ($DcMFc^+PF_6^-$) was synthesized according to a previously described procedure[45] by dissolving 0.2 g of DcMFc in 4 mL of concentrated sulfuric acid. After 1 h, the solution was poured into 60 mL of water. The solution was filtered, and an aqueous solution of KPF_6 was added. The resulting pale green precipitate was filtered, washed

(62) A reviewer suggested that the reaction may also proceed by addition of the alkoxyl radical to the ferrocene donor followed by elimination of the alkoxide anion, a process that is expected to be influenced by a combination of steric and electronic effects. However, this mechanism seems unlikely on the basis of the relatively small increase in reactivity observed on going from $CumO^{\bullet}$ to $BnO^{\bullet}$ where both steric and electronic effects are expected to play in the same direction, as compared to the large increase in reactivity observed on going from *t*-$BuO^{\bullet}$ to $CumO^{\bullet}$, where only electronic effects are expected to operate.

(63) Johnson, R. A.; Nidy, E. G. *J. Org. Chem.* **1975**, *40*, 1680–1681.

with water, and dried under vacuum. A 0.2 g portion of $DcMFc^+PF_6^-$ was obtained (69% yield). The UV−vis spectrum of a 0.1 mM solution of $DcMFc^+PF_6^-$ in CH_3CN is reported in the Supporting Information, Figure S1. The molar extinction coefficient measured at the absorption maximum (λ_{max} = 775 nm) was 589 L mol^{-1} cm^{-1}, in agreement with literature data.[44]

Laser Flash Photolysis Studies. Laser flash photolysis (LFP) experiments were carried out with a laser kinetic spectrometer using the fourth harmonic (266 nm) of a Q-switched Nd:YAG laser, delivering 8 ns pulses. The laser energy was adjusted to ≤10 mJ/pulse by the use of the appropriate filter. A 3 mL Suprasil quartz cell (10 mm ×10 mm) was used for all experiments. Argon- or nitrogen-saturated solutions of di-*tert*-butyl (0.5 M), dicumyl (10−30 mM), and dibenzyl peroxide (8−12 mM) were employed. These peroxide concentrations were chosen in order to ensure, in the presence of the ferrocene donors, prevalent absorption of the 266 nm laser light by the precursor peroxides. All the experiments were carried out at $T = 25 \pm 0.5$ °C under magnetic stirring.

The photochemical stability of the ferrocene donors at the laser excitation wavelength (266 nm) was checked by LFP of acetonitrile solutions containing donor concentrations comparable to the highest concentrations employed in the kinetic experiments. No evidence for the photolytic decomposition of the ferrocene donors and in particular for the formation of the pertinent ferrocenium ions was obtained in these experiments.

First-order or pseudo-first-order rate constants were obtained by averaging four to eight individual values and were reproducible to within 5%.

Second-order rate constants for the reactions of the *tert*-butoxyl (*t*-$BuO^•$), cumyloxyl ($CumO^•$), and benzyloxyl ($BnO^•$) radicals with the ferrocene donors (FcX) were obtained from the slopes of the k_{obs} (measured following the buildup of the ferrocenium ion band between 300 and 330 nm and in the reactions with $CumO^•$ or $BnO^•$ also by following the decay of the visible absorption band at 490 and 460 nm, respectively) vs [FcX] plots. Fresh solutions were used for every ferrocene concentration. Correlation coefficients were in all cases >0.992. The given rate constants are the average of at least two independent experiments, typical errors being <10%.

Acknowledgment. Financial support from the Ministero dell'Istruzione dell'Università e della Ricerca (MIUR) is gratefully acknowledged. We thank Enrico Baciocchi and Flavio Maran for helpful discussion and Lorenzo Stella for the use of a LFP equipment.

Supporting Information Available: Time-resolved absorption spectra observed after reaction of the alkoxyl radicals with alkyl ferrocenes (FcX). Plots of k_{obs} vs [FcX] for the reactions of the alkoxyl radicals. Activation free energies ($\Delta G^{\ddagger}$) for the reactions between $BnO^•$ and FcX. Computational details of the $BnO^•$−DcMFc and *t*-$BuO^•$−DcMFc complexes. Calculated gas-phase and solvent-phase (MeCN) electron affinities for *t*-$BuO^•$, $CumO^•$, and $BnO^•$ and computational details. This material is available free of charge via the Internet at http://pubs.acs.org.